Enhanced performance of $Na_{3.5}Co_4[Bi_2Co_2W_{19.75}O_{70}(H_2O)_6]$/porous graphitic carbon nitride heterojunction based photocatalyst realized by the addition of copper sulfide nanoparticle

Qiushuang Jiang[a, 1], Zhuopeng Liu[a, 1], Xinming Wang[a, *], Huiyuan Ma[a, *], Haijun Pang[a]

a School of Materials Science and Chemical Engineering, Harbin University of Science and Technology, Harbin 150040, PR China.

*Correspondence: wangxinming20@126.com (X. Wang).

Experimental section

1. Materials

Ammonium chloride (NH_4Cl, AR) was purchased from Beijing Hongxing Chemical Factory. Dicyandiamide ($C_2H_4N_4$, AR) and sodium tungstate (Na_2WO_4, AR) were purchased from Shanghai McLean Co., Ltd. Sodium hydroxide (NaOH, AR) and sodium sulfite (Na_2SO_3, AR) were purchased from Shanghai Yien Chemical Technology Co., Ltd. Glacial acetic acid (CH_3COOH, AR) and absolute ethyl alcohol (C_2H_5OH, AR) were purchased from Tianjin Fuyu Fine Chemical Co., Ltd. Bismuth nitrate ($Bi(NO_3)_3$, AR) was purchased from Shanghai Luoen Co., Ltd. Concentrated nitric acid (HNO_3, AR) was purchased from Xilong Chemical Co., Ltd. Cobaltous acetate ($Co(CH_3COO)_2{\cdot}4H_2O$, AR), copper chloride ($CuCl_2$, AR) and sodium sulfide (Na_2SO_4, AR) were purchased from Tianjin Guangfu Technology Development Co., Ltd. Sodium citrate ($Na_3C_6H_5O_7{\cdot}2H_2O$, AR) and Nafion($C_9HF_{17}O_5S$, AR) were purchased from Sigma-Aldrich. Sodium sulfate (Na_2S, AR) was purchased from Fuchen Chemical Reagent Co., Ltd. All samples were used without further purification. The deionized (DI) water was produced using an ultrapure water system.

2. Photocatalytic Hydrogen Production

The photocatalytic H_2 evolution experiment was tested by an off-line photocatalytic test system and a gas spectrometer, the light source was a 300 W xenon lamp, the hydrogen was detected by a GC9800 gas chromatograph, and the detector was a TCD thermal conductivity detector. The photocatalytic reaction was carried out in a 30 mL quartz reaction vessel with high-purity nitrogen as the carrier gas. In a typical procedure, the reaction system was filled with condensate to keep the temperature at 4 ℃, photocatalysts (5 mg) were uniformly distributed in 0.35 M Na_2S

/ 0.25 M Na_2SO_3 aqueous solution (20 mL). After degassing with inert N_2 for 30 min, the reaction system was illuminated by a 300 W xenon lamp, and stirred to make the reaction system reach a homogeneous state. The photocatalytic hydrogen production was tested every hour, and 200 μL of gas was extracted from the reaction system each time. The stability of photocatalytic hydrogen production was tested under above conditions for 30 h.

According to the comment, we have calculated Turnover number (TON) and Turnover frequency (TOF) for photocatalytic H_2 production activity of BiWCo/CuS/PGCN. The TON and TOF can be calculated from the following equations:

$$\text{TON (Turnover Number)} = \frac{\text{number of evolved H2 molecules}}{\text{number of catalyst molecules}} = \frac{\text{n(H2)}}{\text{n(catalyst)}}$$

$$\text{TOF (Turnover Frequency)} = \frac{\text{TON}}{\text{reaction time (h)}}$$

3. Photoelectrochemical measurements

CHI760E electrochemical workstation was employed to measure transient photocurrent response, electrochemical impedance spectra (EIS) and Mott-Schottky (M-S) plot test. In typical experiments, sample, Ag/AgCl (in saturated KCl) and Pt plate acted as working electrode, reference electrode and counter electrode, respectively, with Na_2SO_4 aqueous solution (0.3 M) as electrolyte. As for the working electrode, the synthesized sample (5 mg) was added to a mixed solution of 1 mL CH_3CH_2OH and 20 μL Nafion, and the working electrode was prepared by dropping the suspension (200 μL) onto the electrode surface of an ITO glass substrate and dried at room temperature.

4. Characterization

The X-ray diffraction (XRD) patterns were recorded from a PANalytical X'pert MPD Pro diffractometer with Ni-filtered Cu Kα irradiation at a scan rate of 5°/min and a 2θ range of 5° to 80°. Fourier transform infrared spectroscopy (FIIR) spectra were recorded from KBr particles in the 4000-500 cm^{-1} range using a TENSOR II spectrometer. The morphology of the samples was analyzed using scanning electron microscopy (SEM, SIGMA300) and transmission electron microscopy (TEM, JEM-2100). Before the SEM test, the samples were sprayed with gold on the conductive adhesive, and then the morphology was observed. Prior to TEM testing, the test samples were ultrasonically dispersed in ethanol and dropped onto a copper mesh with a carbon film. High-resolution TEM (HRTEM) was absorbed using 200 KV FEI-Tecnai G2 20 S-TWIN High Resolution Transmission Electron Microscope. Field emission scanning electron microscopy (FESEM) experiments were carried out at 20 KV by means of a Hitachi S4160 (Cold Field Emission) analyzer. Energy dispersive spectroscopy (EDS) data was collected with an ensemble measurement in the FESEM. The nitrogen adsorption isotherm (NOVA2000e) was utilized to measure the specific surface area and pore size distribution. X-ray photoelectron spectroscopy (XPS) measurements were performed on a Thermo ESCALAB 250Xi spectrometer with monochromatic Al Kα radiation (hγ = 1486.6 eV). The C 1s peak at 284.8 eV of surface adventitious carbon was applied for calibration. Optical properties were evaluated by diffuse reflectance ultraviolet–visible (UV–vis, Hitachi UV–3600i PLUS) spectroscopy. And steady-state photoluminescence (PL) spectra were collected utilizing an Edinburgh FLS1000 with an excitation wavelength of 270 nm and the wavelength range was 200-800 nm.

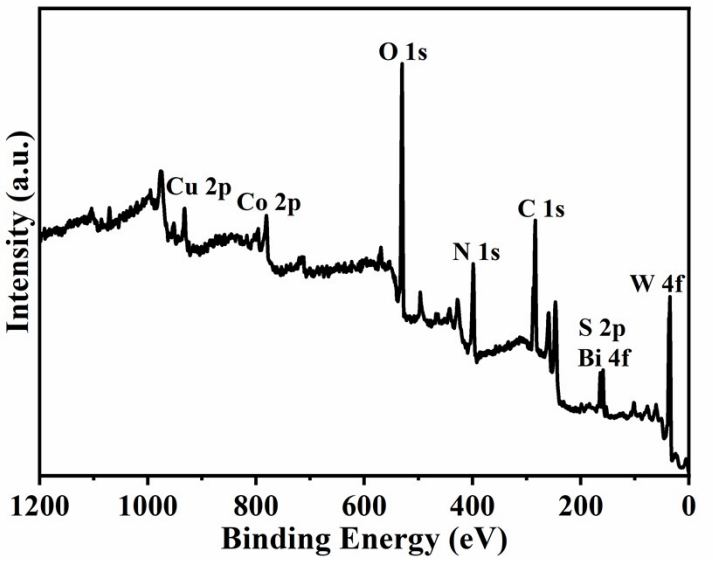

Fig. S1. XPS survey spectra of BiWCo/CuS/PGCN.

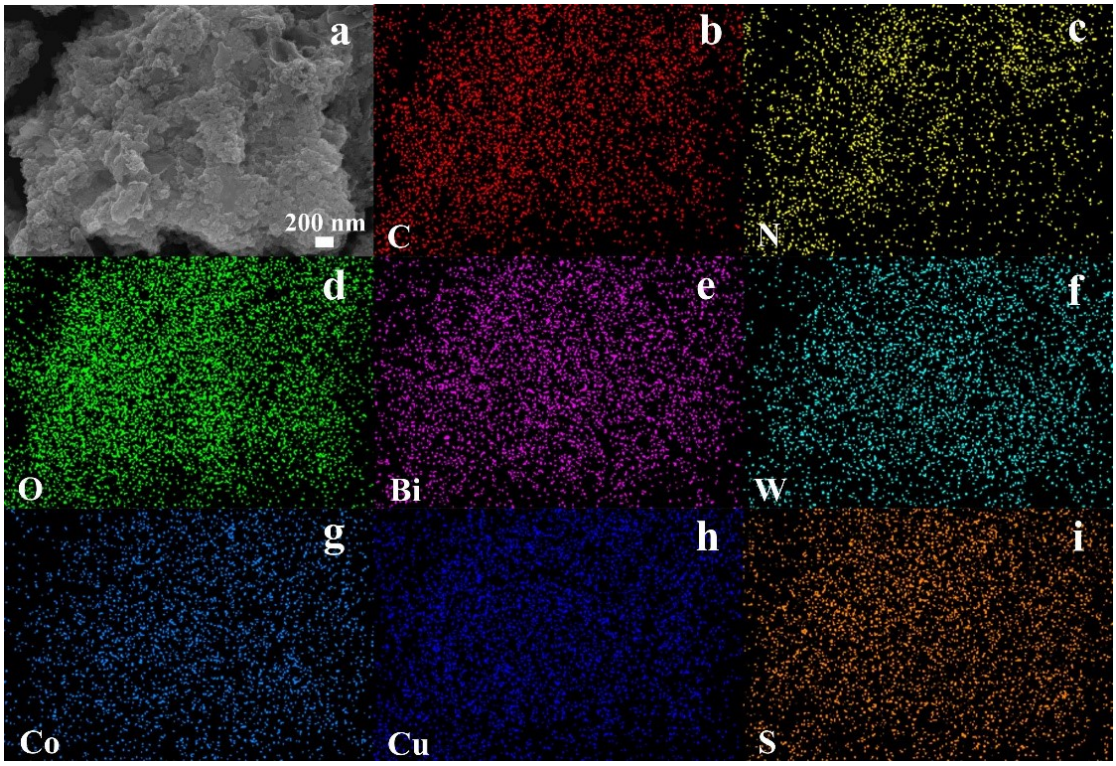

Fig. S2. The SEM image of BiWCo/CuS/PGCN (a) and the elemental mapping images of C (b), N (c), O (d), Bi (e), W (f), Co (g), Cu (h) and S (i) for BiWCo/CuS/PGCN.

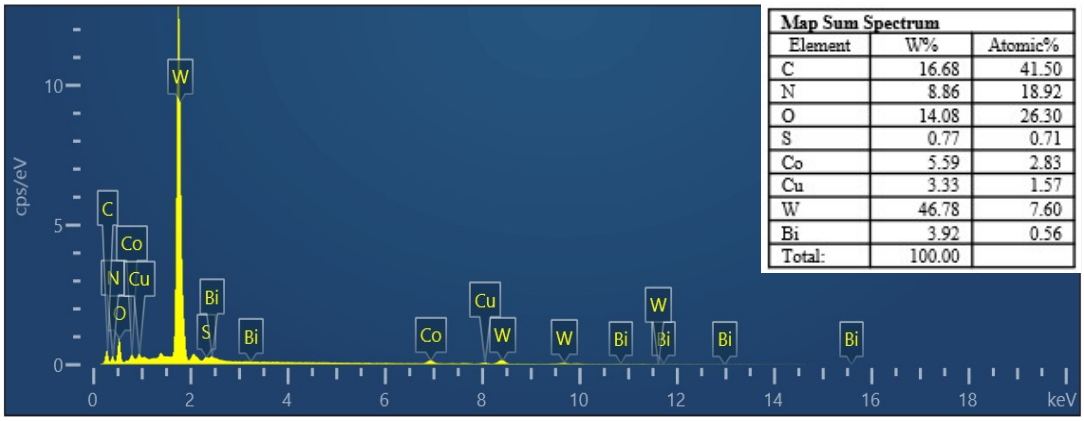

Map Sum Spectrum		
Element	W%	Atomic%
C	16.68	41.50
N	8.86	18.92
O	14.08	26.30
S	0.77	0.71
Co	5.59	2.83
Cu	3.33	1.57
W	46.78	7.60
Bi	3.92	0.56
Total:	100.00	

Fig. S3. The EDS spectrum of BiWCo/CuS/PGCN.

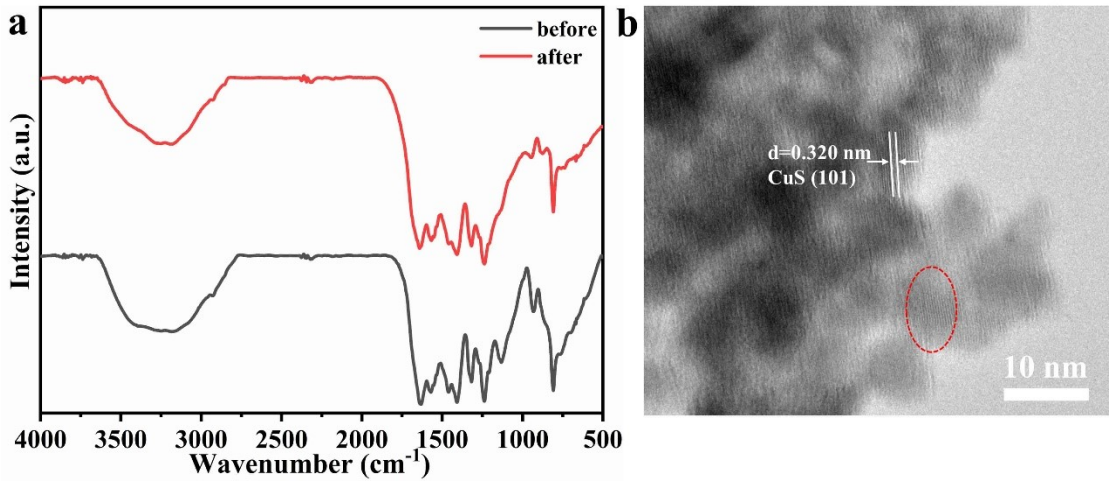

Fig. S4. The FT-IR spectra and the TEM image of BiWCo/CuS/PGCN after 30 h illumination.

Table S1 Comparison of hydrogen production performance of some polyoxometalate-based photocatalytic composite materials.

Materials	Hole scavenger	Co-catalyst	Hydrogen production rate ($\mu mol\ g^{-1}\ h^{-1}$)	Ref.
NS-CN	TEOA	0.03 wt% Pt	571.01	[1]
Porous g-C_3N_4	CH_3OH	3.0 wt% Pt	1305.90	[2]
PW_{12}@UiO-NH_2	CH_3OH	-	72.7	[3]
SiW_{12}/C_3N_4-3	TEOA	1.0 wt% Pt	2400.00	[4]
$Nb_6/Cd_{0.5}Zn_{0.5}S$/g-C_3N_4	Na_2S/Na_2SO_3	-	1777.86	[5]
$Bi_2WO_6/C_3N_4/Ti_3C_2$	TEOA	-	54.4	[6]
Nb_6/PPy-RGO	CH_3OH	-	207.60	[7]
NiS/CuS/C_3N_4	TEOA	NiS	1602.00	[8]
g-C_3N_4-PANI-MoS_2	TEOA	-	594.00	[9]
TiO_2-Si-NH_2-$PW_{11}Pt_2$	CH_3OH	-	4500.00	[10]
BiWCo/CuS/PGCN	**Na_2S/Na_2SO_3**	**CuS**	**3477.58**	**This Work**

References

[1] M. Rahman, J. Ran, Y. Tang, M. Jaroniec, S. Qiao, Surface activated carbon nitride nanosheets with optimized electro-optical properties for highly efficient photocatalytic hydrogen production, J. Mater. Chem. A 4 (2016) 2445-2452.

[2] L. Tang, Z, Chen, G, Chen, F. Zuo, B. Hua, L. Zhang, J. Li, Y. Sun, CaH_2-assisted structural engineering of porous defective graphitic carbon nitride (g-C_3N_4) for enhanced photocatalytic hydrogen evolution, Int. J. Hydrogen Energy 45 (2020) 18937-18945.

[3] P. Tian, X. He, W. Li, L. Zhao, W. Fang, H. Chen, F. Zhang, W. Zhang, W. Wang, Zr-MOFs based on Keggin-type polyoxometalates for photocatalytic hydrogen production, J. Mater. Sci. 53 (2018) 12016-12029.

[4] G. Yan, X. Feng, L. Xiao, W. Xi, H. Tan, H. Shi, Y. Wang, Y. Li, Tuning of the photocatalytic performance of g-C_3N_4 by polyoxometalates under visible light, Dalton Trans. 46 (2017) 16019-16024.

[5] X. Zhou, D. Zhao, X. Li, Y. Sun, S. Zheng, Synthesis of noble-metal-free ternary $K_7HNb_6O_{19}/Cd_{0.5}Zn_{0.5}S/g\text{-}C_3N_4$ tandem heterojunctions for efficient photocatalytic performance under visible light, Appl. Organomet. Chem. 33 (2019) e5178.

[6] K. Wu, S. Song, H. Wu, J. Guo, L. Zhang, Facile synthesis of $Bi_2WO_6/C_3N_4/Ti_3C_2$ composite as Z-scheme photocatalyst for efficient ciprofloxacin degradation and H_2 production, Appl. Catal. A Gen. 608 (2020) 117869.

[7] S. Heng, L. Li, W. Li, H. Li, J. Pang, M. Zhang, Y. Bai, D. Dang, Enhanced photocatalytic hydrogen production of the polyoxoniobate modified with RGO and PPy, Nanomaterials 10 (2020) 2449.

[8] Y. Xu, C. Du, C. Zhou, S. Yang, Ternary noble-metal-free heterostructured NiS–CuS–C_3N_4 with near-infrared response for enhanced photocatalytic hydrogen evolution, Int. J. Hydrogen Energy 45 (2020) 4084-4094.

[9] T. Li, J. Cui, L. Gao, Y. Lin, R. Li, H. Xie, Y. Zhang, K. Li, Competitive self-assembly of PANI confined MoS_2 boosting the photocatalytic activity of the graphitic carbon nitride, ACS Sustain. Chem. Eng. 8 (2020) 13352-13361.

[10] Y. Cao, D. Yin, M. Wang, T. Pang, Y. Lv, B. Liu, G. Gao, L. Ma, H. Liu,Pt-Substituted polyoxometalate modification on the surface of low-cost TiO_2 with highly efficient H_2 evolution performance, Dalton Trans. 49 (2020) 2176-2183.